

Fiber-optic pressure sensors for internal combustion engines

R. A. Atkins, J. H. Gardner, W. N. Gibler, C. E. Lee, M. D. Oakland, M. O. Spears, V. P. Swenson, H. F. Taylor, J. J. McCoy, and G. Beshouri

Two designs incorporating embedded fiber Fabry-Perot interferometers as strain gauges were used for monitoring gas pressure in internal combustion engines. Measurements on a Diesel engine, a gasoline-fueled engine, and a natural-gas engine are reported.

The need for improved pressure sensors is widely recognized in the engine research and development community. The ideal sensor would give accurate readings of the combustion chamber gas pressure with high temporal resolution within each engine cycle. It would also operate reliably for several years, and for at least one year without recalibration, and be inexpensive. Such sensors could be utilized in engine control systems for improving fuel economy and reducing harmful emission levels. They could also find application in improved instrumentation for engine research and development, e.g., for accurate determination of heat-release rates.

Dynamic information on gas pressure in automobile and truck engines and in smaller engines is difficult to obtain because suitable transducers are not available. In some large engines a port in the cylinder wall or head is provided for pressure measurement. Gas that exits the combustion chamber through this port passes through a metal tube to a spring-activated pressure gauge. This gauge is located remotely from the combustion chamber because it cannot operate reliably at high temperatures. The slow response of such sensors tends to limit their utility to average pressure measurements, and these data are sometimes suspect because of errors that are

due to acoustical effects and pressure drop in the tube.

More accurate pressure readings with acceptable time resolutions are provided by piezoelectric transducers mounted in a special port, usually in the cylinder head. Two types of transducer are used. In one type a piezoelectric element is directly exposed to the pressure; in the other a strain gauge responds to a displacement in a piston exposed to the pressure.¹ These transducers must be cooled by circulating air or water because of the high-temperature environment in which they operate. Even then, frequent calibration is required, operating life is short, and the sensors are expensive. Piezoelectric pressure transducers have proved useful in engine research and development but have not been widely incorporated into engine products.

Fiber-optic sensors represent an emerging alternative to piezoelectric sensors for in-cylinder pressure measurements, since the optical sensors are not affected by extreme temperatures that cause rapid degradation or destruction of piezoelectric devices. Fiber-optic sensors have operated continuously at temperatures above 1000 °C (Ref. 2) versus a maximum allowable temperature of 250 °C for uncooled piezoelectric pressure sensors. Engine pressure monitoring with an extrinsic fiber sensor by utilizing a diaphragm near the end of a multimode fiber has been reported.³ To the best of our knowledge the first results on the application of intrinsic fiber-optic sensors in the measurement of combustion chamber pressure are described in this paper.

The sensing element is a fiber Fabry-Perot interferometer (FFPI) fabricated in single-mode fiber.⁴ The pressure is determined from the optical signal from the FFPI, which is a sensitive strain transducer.⁵ The FFPI consists of two internal mirrors separated

R. A. Atkins, J. H. Gardner, W. N. Gibler, C. E. Lee, M. D. Oakland, M. O. Spears, V. P. Swenson, and H. F. Taylor are with the Department of Electrical Engineering, Texas A&M University, College Station, Texas 77843. J. J. McCoy is with Tenneco Gas, P.O. Box 2511, Houston, Texas 77252. G. Beshouri is with the Advanced Engine Technologies Corporation, 16636 Kildare Road, San Leandro, California 94578.

Received 25 January 1993; revised manuscript received 7 June 1993.

0003-6935/94/071315-06\$06.00/0.

© 1994 Optical Society of America.

by a length L of fiber, as illustrated in Fig. 1. Each mirror is produced by vacuum deposition of a thin film of the dielectric material TiO_2 on the cleaved end of a fiber.² A fusion-splicing technique integrates the mirrors into a continuous length of the fiber. The reflectance R of the mirrors used in the FFPI's for the pressure sensors described here is in the 2-4% range.

In the case of a lossless interferometer with mirrors of reflectance R_1 and R_2 , where R_1 and $R_2 \ll 1$, it is easily shown that the reflectance of the interferometer, R_{FP} , can be written as

$$R_{\text{FP}} = R_1 + R_2 + 2(R_1 R_2)^{1/2} \cos \phi, \quad (1)$$

with ϕ , the round-trip phase shift in the interferometer, given by

$$\phi = 4\pi n L \nu / c, \quad (2)$$

where ν is the optical frequency, n is the effective refractive index of the fiber mode, and c is the free-space velocity of light. By measuring the reflected optical power one can determine the value of the parameter of interest. Only perturbations that affect the fiber in the region between the mirrors are sensed. If the induced change in nL for the FFPI is proportional to combustion chamber pressure P , then

$$\phi \approx \phi_0 + KP, \quad (3)$$

where ϕ_0 is the round-trip phase shift at zero pressure and K is a constant that depends on the sensor configuration.

Two designs for the pressure sensor, illustrated schematically in Fig. 2, have been investigated. In both designs, the FFPI functions as a strain gauge. In the first design [Fig. 2(a)] the FFPI is embedded in a hole drilled along the axis of a bolt that was used to attach a fuel injector valve, which is directly exposed to the combustion chamber pressure, to the cylinder head. The bolt experiences a longitudinal strain in response to the pressure. In the second design [Fig. 2(b)] the FFPI is embedded in a metal rod in contact with one or more metal diaphragms that are exposed to the pressure. In this case the pressure causes a longitudinal compression of the rod and hence the embedded FFPI.

The arrangement shown in Fig. 3 is used for monitoring a FFPI pressure sensor.⁵ Light from a continuously operating 1.3- μm semiconductor laser diode is coupled into a single-mode optical fiber. The temperature of the laser heat sink is controlled with a

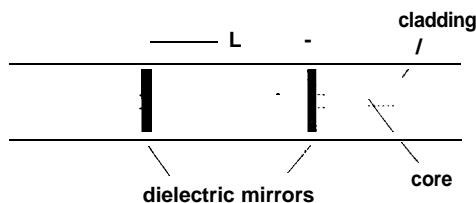


Fig. 1. Fiber Fabry-Perot interferometer.

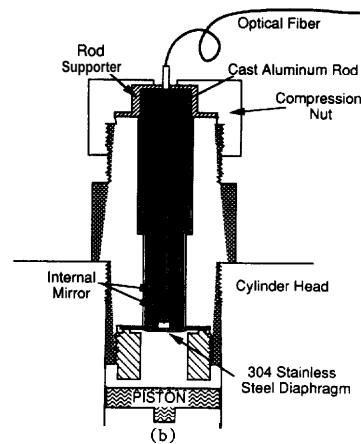
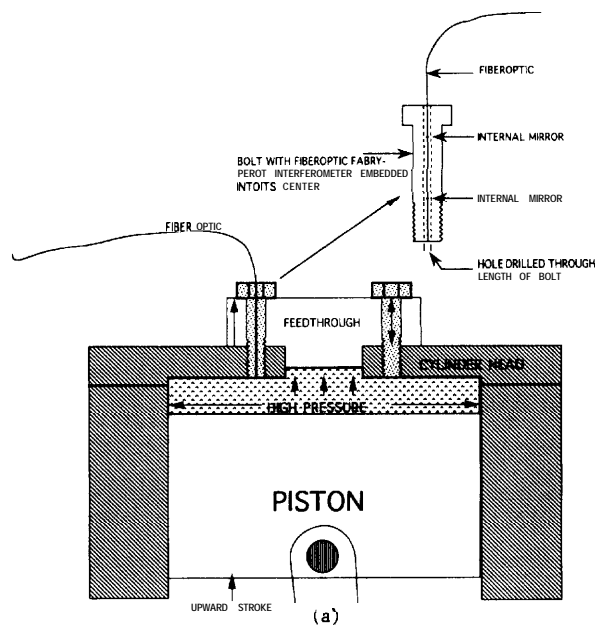


Fig. 2. Designs for the fiber-optic pressure sensor: (a) the FFPI is embedded in a bolt that attaches the fuel injector valve to the cylinder head; (b) the FFPI is embedded in a metal rod in contact with metal diaphragms that are exposed to the combustion chamber pressure.

thermoelectric cooler and monitored with a thermistor. After passing through an optical isolator and a fiber coupler that splits the light into two equal-amplitude components, a portion of the light is reflected from the FFPI. After passing through the coupler once again, the light modulated by the FFPI

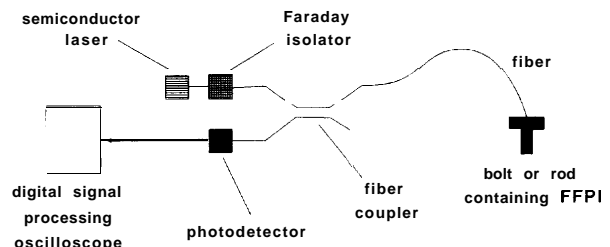


Fig. 3. Experimental arrangement for monitoring a pressure sensor.

is converted by an InGaAs photodiode to an electrical signal that is displayed on an oscilloscope.

The laser frequency is controlled in order to obtain linear operation of the sensor. It is evident from Eq. (1) and approximation (3) that in general the interferometer reflectance is a nonlinear function of the pressure. However, for small dynamic pressure variations, the reflectance is close to a linear function of the pressure if $\phi_0 \approx m\pi + \pi/2$, with m an integer. These values of ϕ_0 also represent the regimes in which the reflectance is most sensitive to small pressure changes. In practice one can adjust ϕ_0 to one of these quasi-linear operating regimes by thermal tuning of the laser. The laser frequency is a strong function of temperature, and from Eq. (2) it is evident that ϕ_0 is proportional to v .

Initial experiments were carried out in a 5-hp, single-cylinder Diesel engine. A 4-mm-long FFPI was embedded with high-temperature epoxy in a hole drilled in one of two bolts that were used to attach the fuel injector valve to the cylinder head, as in Fig. 2(a). This valve is directly exposed to the combustion chamber environment. Pressure in the chamber produces an axial strain in the bolt, which is also experienced by the embedded fiber sensor. Figure 4 shows data that compare the fiber sensor signal with that from a conventional piezoelectric pressure sensor. The water-cooled piezoelectric sensor is mounted in a special port in the cylinder head and is directly exposed to the combustion chamber environment. The laser temperature was adjusted to obtain operation in the quasi-linear region between the minimum and maximum reflectance values indicated by the cursors. The oscillations that are evident in the FFPI data, and particularly in that of Fig. 4(a), are believed to represent acoustic pickup by the fiber-optic sensor corresponding to mechanical resonances in the engine at a frequency near 2 kHz. Figure 5 compares the piezoelectric sensor output with the corrected pressure values computed from the relation

$$P = \cos^{-1}[(I_{FP} - I_{\max})/(I_{\max} - I_{\min})]/K - \phi_0/K, \quad (4)$$

derived from Eq. (1) and approximation (3), where I_{FP} is the photocurrent from the FFPI sensor and I_{\max} and I_{\min} are the maximum and minimum photocurrents. It is assumed in Eq. (4) that the photocurrent is proportional to the interferometer reflectance. In the plot of Fig. 5, the scale factor K is adjusted to match the pressure excursion (difference between maximum and minimum pressure) for the optical and piezoelectric sensors. Except for the high-frequency

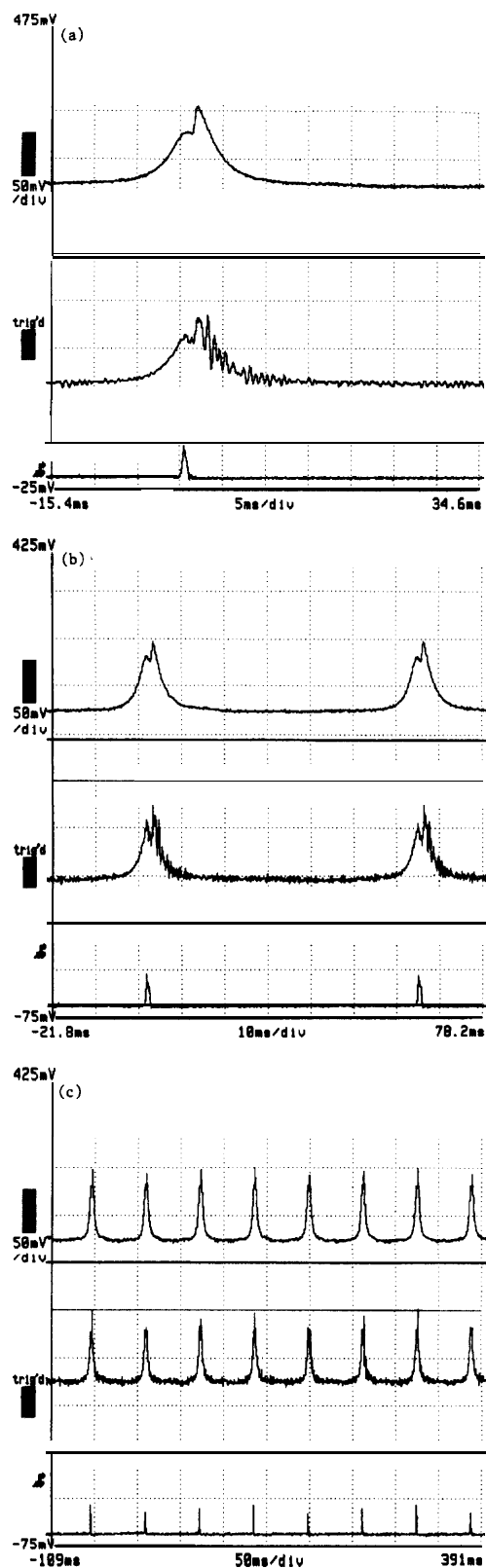


Fig. 4. Oscilloscope traces of sensor output from a Diesel engine operating at 950 rpm: horizontal scale: (a) 5 ms/division, (b) 10 ms/division, (c) 50 ms/division. In each case the upper trace is the piezoelectric sensor output, the middle trace is the FFPI output, and the lower trace indicates the top dead center position of the piston. The cursors above and below the FFPI trace indicate the maximum and minimum signals from the photodetector as determined by thermal tuning of the laser.

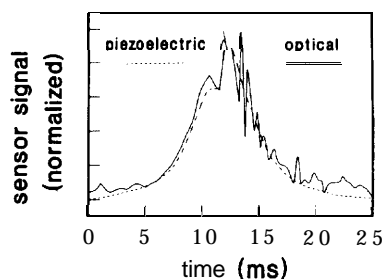


Fig. 5. Comparison of pressure determined from a piezoelectric sensor with the linearized output of the FFPI by using the oscilloscope plot of Fig. 4(a).

oscillations, agreement between the two sensors is quite close.

The FFPI is highly sensitive to temperature as well as to strain. Thus it was observed that, with the laser temperature held constant, the operating point of the interferometer traverses a number of fringes from the time the engine is started until steady-state operation is reached. However, since the fiber sensor is mounted ~ 7 cm from the combustion chamber, the time required for the heat to diffuse through the metal from the combustion region to the sensor is sufficiently large (> 1 s) that transient thermal effects are avoided.

A second sensor design utilizes an aluminum rod in which an FFPI was embedded, as in Fig. 2(b). The FFPI was positioned in a graphite mold into which molten aluminum alloy 356 (92.7% Al, 7% Si, 0.3% Mg) was poured. A stainless-steel tube through which the fiber passes into the rod prevents breakage of the fiber during the casting process and provides strain relief in the finished part.⁷ One or more stainless-steel diaphragms exposed to the combustion chamber pressure were pressed into contact with the cylinder by using a threaded fitting. In this case the combustion chamber pressure induces a compressional strain in the FFPI sensor.

A small (2-hp) gasoline-powered engine was used for the initial test of this design. In order to provide a greater range of operating conditions we connected the engine as the power source for a water pump for which the load (water pressure) could be adjusted with a valve. Some typical results are shown in Fig. 6 for a sensor with a FFPI length of 12 mm. At low revolutions per minute and load, the sensor output is a monotonic function of gas pressure, as in Fig. 6(a). At high revolutions per minute and load [Fig. 6(b)] the nonlinear response of the FFPI is evident from the observation that for some of the ignitions the peak pressure corresponds to a minimum rather than a maximum in the optical signal. One can understand this behavior by referring to Eq. (1) and approximation (3), which show that for large enough phase shift the optical response R_{FP} is no longer a monotonic function of P . Thus when the phase excursion exceeds $\pi/2$ rad, it is impossible for one to maintain quasi-linear operation by controlling the laser temperature.

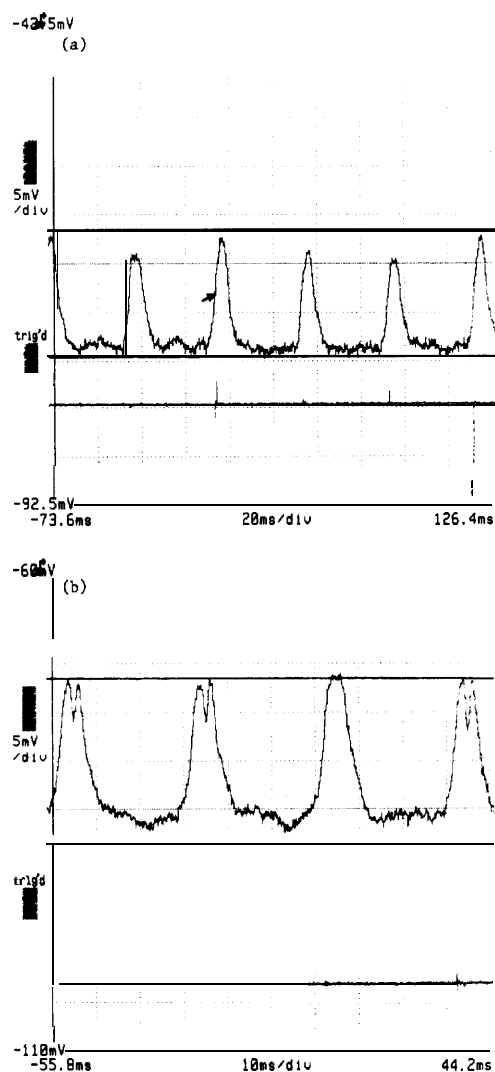


Fig. 6. Oscilloscope traces of sensor output from a gasoline-powered engine: (a) revolution rate, 1500 rpm, load, 50 psi, with diaphragms in place; (b) revolution rate, 2000 rpm, load, 150 psi, with diaphragms. In each case the upper trace is the FFPI output, and the lower trace is electrical pickup from the spark plug. The cursors above and below the FFPI trace indicate the maximum and minimum signals from the photodetector as determined by thermal tuning of the laser.

Another sensor with the design of Fig. 2(b) was tested in a cylinder of a large (1500-hp) eight-cylinder natural-gas-fueled engine in a natural-gas pipeline pumping station. Dynamic response of the fiber-optic pressure sensor is shown in Fig. 7 after 3 h of in-cylinder operation. The sensor response indicated here was not noticeably different from that observed at the beginning of the test period.

A simple model can be applied to estimate the optical phase shift for comparison with the experimental results of Figs. 4-7. The strain ϵ_z along the z axis in a uniform material with Young's modulus E and cross-sectional area A_0 produced by pressure P applied to an area A_p is given by

$$\epsilon_z = -A_p P / (A_0 E), \quad (5)$$

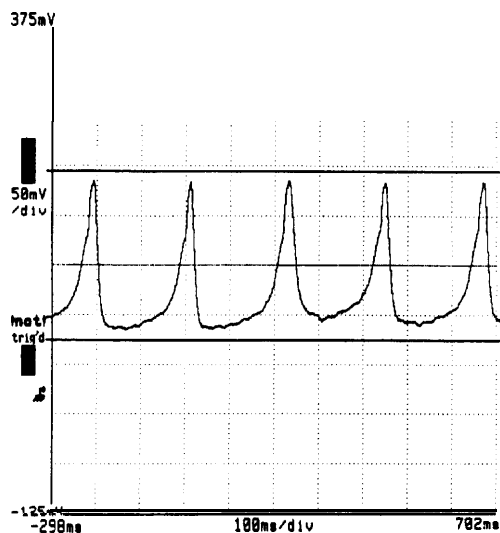


Fig. 7. Oscilloscope traces of sensor output from a natural-gas-powered engine operating at 275 rpm. The cursors indicate the maximum and minimum signals from the photodetector as determined by thermal tuning of the laser.

whereas the radial strain is $-\mu\epsilon_z$. The refractive-index change in a fiber for light polarized perpendicular to the axis is

$$\Delta n = -n^3(p_{12} - \mu p_{11} - \mu p_{12})\epsilon_z/2, \quad (6)$$

where p_{11} and p_{12} are the strain-optic coefficients for the fiber material.⁸ The round-trip phase shift in a FFPI of length L is given by Eq. (2), and it is evident from Eq. (6) that the change in this phase shift caused by longitudinal strain is

$$\Delta\phi \approx (4\pi nL\nu/c)\epsilon_z[1 - n^2(p_{12} - \mu p_{11} - \mu p_{12})/2]. \quad (7)$$

When $n = 1.46$, $\mu = 0.17$, $p_{11} = 0.12$, and $p_{12} = 0.27$ for a silica fiber,⁷

$$A_+ \approx 0.78(4\pi nL\nu/c)\epsilon_z. \quad (8)$$

Combining this result with Eq. (5) makes it possible to express the constant K in approximation (3), which relates the phase shift to the pressure for the FFPI, in the form

$$K = -3.12\pi nL\nu A_p / (cA_0 E). \quad (9)$$

The results of the engine tests are summarized in Table 1. The value of K used to relate the measured phase shift to the pressure for each sensor was

determined from Eq. (9) by using the parameter values given in Table 1. The optical frequency ν that corresponds to the laser wavelength of $1.3 \mu\text{m}$ is 2.31×10^{14} Hz. The phase shift excursion during a cycle of the engine $\phi_{\text{max}} - \phi_{\text{min}}$ was determined from the data of Figs. 4, 6, and 7 and Eq. (4). The pressure excursion $P_{\text{max}} - P_{\text{min}}$ was then calculated by using approximation (3). The $P_{\text{max}} - P_{\text{min}}$ values in Table 1 should be regarded as only a rough estimate since the model used to derive Eq. (9) is a greatly simplified representation of a complex problem in mechanics.

In conclusion, two designs for fiber-optic pressure sensors utilizing FFPI's as strain gauges have been successfully tested in internal combustion engines. In one design the FFPI is embedded in a bolt that attaches the fuel injector valve to the cylinder head in a Diesel engine. In the other design the FFPI is embedded in an aluminum rod in contact with steel diaphragms that are directly exposed to the combustion chamber pressure. By controlling the temperature of the semiconductor laser that was used as the light source for the sensor, it was possible to adjust the operating point of the interferometer to the quasi-linear operating region for both sensor designs. In the Diesel engine tests, the bolt-mounted FFPI sensor yielded results similar to those obtained with a conventional piezoelectric sensor, except that the FFPI sensor output exhibited an oscillatory waveform at ≈ 2 kHz superimposed on the pressure response. This spurious output from the sensor, evidently caused by an acoustic wave that corresponds to a mechanical resonance of the engine, can be suppressed by low-pass filtering of the optical sensor waveform. The diaphragm sensor design was successfully tested in gasoline-powered and natural-gas-fueled engines, and the data were found to be free of transient oscillations. It has been shown that the fiber sensors can respond rapidly (response time < 1 ms) to pressure variations in the engine. Since the FFPI's have operated continuously at temperatures > 1000 °C, they are expected to be more reliable than piezoelectric or strain gauge pressure sensors in a high-temperature engine environment. This could lead to a number of new applications in engine control and in engine research and development.

The authors express appreciation to T. Lalk of the Mechanical Engineering Department at Texas A&M for helpful advice, and to J. A. Caton of that Depart-

Table 1. Summary of Engine Test Results^a

Engine	Data Source (Fig.)	L (cm)	A_p (cm ²)	A_0 (cm ²)	E (m ² /N)	K (rad/pA)	$\phi_{\text{max}} - \phi_{\text{min}}$ (rad)	$P_{\text{max}} - P_{\text{min}}$ (pA)
Diesel	4	0.4	3.5	0.67	2×10^{11}	6.5×10^{-7}	0.71	1.08×10^6
Gasoline	6(a)	1.2	0.38	0.27	7×10^{10}	1.82×10^{-6}	1.70	9.3×10^5
Gasoline	6(b)	1.2	0.38	0.27	7×10^{10}	1.82×10^{-6}	3.55	1.95×10^6
Natural gas	7	1.2	0.38	0.27	7×10^{10}	1.82×10^{-6}	1.97	1.08×10^6

^a1 pA = $1 \text{ N/m}^2 = 9.87 \times 10^{-6} \text{ atm} = 1.45 \times 10^{-4} \text{ psi}$.